Global Journal of Pure and Applied Mathematics.
ISSN 0973-1768 Volume 11, Number 5 (2015), pp. 3805-3821

http://www.ripublication.com/gjpam.htm

Finite Element Solutions Using Hybrid of Block-Pulse Functions and Lagrange Polynomial

Murugesan Indu Bharathy and V. Prabhakar[1]
School of Advanced Sciences,
VIT University, Chennai Campus,
Vandalur-Kelambakkam Road, Chennai- 600127,
Tamil Nadu, India
E-mail: murugesan.indu2013@vit.ac.in; prabhakar.v@vit.ac.in

Abstract

An attempt is made to obtain the Finite Element Solutions to steady state and transient state heat conduction problems using the hybrid of Block-Pulse functions and Lagrange interpolation polynomial. This method can be used to obtain accurate results. The finite element results are compared with the corresponding results obtained using quadrature methods and found to be in good agreement.

AMS subject classification:
Keywords: Finite element method, Hybrid function, Block-pulse function, Lagrange polynomial, Quadrature method, Heat conduction.

1. Introduction

Finite Element Method (FEM) is a computer-aided numerical technique used to solve wide range of problems in engineering and sciences, wherein, the variables are related by means of algebraic, differential and integral equations. The method is very efficient in dealing with complex geometries and unstructured domains. As the complexity increases, the integration procedure to calculate the elements of the stiffness and mass matrices associated with the finite element equations becomes more complicated. Usually, Gaussian quadrature method is used as a standard tool for determining the elements of these matrices.

Siraj-ul-Islam et al. [1], considered a comparative study of quadrature rule based on Haar Wavelet and Hybrid function of block-pulse and Legendre polynomial for finding

[1]Corresponding Author.

the approximate value of the definite integrals and extended the procedure for the numerical solution of double and triple integrals with variable limits. They have concluded that the main advantage of the hybrid method is its efficiency, simple applicability, faster convergence than the Haar Wavelet and that the order of the block-pulse functions and Legendre polynomial can be adjusted to obtain highly accurate solution. In their paper, Uma et al. [2] considered Hybrid of Block-Pulse function using Lagrange basis polynomial for the evaluation of general double and triple integrals with variable limits which shows better accuracy than the Haar Wavelet. They have considered variable weights for their study in contrast with the constant weights considered in Siraj-ul-Islam et al. [1]. This approach is summarized in Section 2.

Marzban et al. [3] proposed a numerical method based on the Hybrid function approximations for solving nonlinear initial-value problems with applications to Lane-emden type equations. They utilized the properties of block-pulse functions and Lagrange interpolating polynomials to reduce the nonlinear initial-value problem to a system of non-algebraic equations, and obtained accurate results. The same method was also used to provide accurate results for solving nonlinear integro-differential equations such as in Volterra's population model [4] and Volterra-Fredholm equation [5], and also for variational problems in Marzban et al. [6].

Motivated by these, the present paper attempts to consider the Hybrid function based on the Block-Pulse function and Lagrange basis polynomial for the numerical integration technique instead of the quadrature method for obtaining accurately the finite element solutions. They are illustrated using a few examples on heat transfer problems in 1-D, 2-D and 3-D for steady state and transient problems and the results are presented. The method is easy to implement and computationally very attractive.

The structure of the paper is as follows: Section 2 gives the short description of the hybrid of the block-pulse and Lagrange polynomials. Section 3 provides the finite element results for the heat transfer applications obtained using hybrid functions. Finally, conclusions are drawn in Section 4.

2. Preliminaries

2.1. Block-Pulse Function

A set of block-pulse function $\phi_n(t), n = 1, 2, \ldots, N$ defined on the interval [0, 1) are denoted as

$$\phi_n(t) = \begin{cases} 1 & t_{n-1} \leq t \leq t_n \\ 0 & Otherwise \end{cases} \tag{2.1}$$

Here $\left[t_{n-1}, t_n\right)$ denotes the n^{th} partition and N represents the number of partitions of [0, 1).

2.2. Hybrid functions of Block-Pulse and Lagrange basis polynomials

A set of hybrid functions $s_{nm}(t), n = 1, 2, \ldots N, m = 0, 1, \ldots M-1$, on the interval [0, 1) are denoted as

$$s_{nm}(t) = \begin{cases} L_m(2Nt - 2n + 1) & t \in \left[\frac{n-1}{N}, \frac{n}{N}\right] \\ 0 & Otherwise \end{cases} \tag{2.2}$$

Here the Lagrange basis polynomial, $L_m(t)$ is denoted by

$$L_m(t) = \prod_{i=0, i\neq m}^{M-1} \frac{t - \tau_i}{\tau_m - \tau_i} \tag{2.3}$$

with $\tau_i, i = 0, 1, \ldots, M-1$, being the roots of the Legendre polynomial of order M, with the Kronecker delta property

$$L_m(\tau_i) = \delta_{mi} = \begin{cases} 1 & i = m \\ 0 & i \neq m \end{cases} \tag{2.4}$$

It may be noted that M denotes the number of interior points in each partition of the interval (0, 1].

As the block-pulse functions and Lagrange interpolating polynomials are complete and orthogonal, the set of hybrid functions $\{s_{nm}(t)\}$ is a complete orthogonal set in the Hilbert Space $L^2[0, 1)$.

2.3. Function Approximation using Hybrid function

A function $f(t) \in L^2[0, 1)$ can be approximated, in terms of the hybrid function, as

$$f(t) = \sum_{n=1}^{\infty} \sum_{m=0}^{\infty} c_{nm} s_{nm}(t) \tag{2.5}$$

In practice

$$f(t) \approx \sum_{n=1}^{N} \sum_{m=0}^{M-1} c_{nm} s_{nm}(t), n = 1, 2, \ldots, N, m = 0, 1, \ldots, M-1 \tag{2.6}$$

For a fixed N and M, the number of nodes considered for the function approximation is NM. To find the co-efficients c_{nm}, consider the Gaussian nodes r_{nm} of the n^{th} subinterval $\left[\frac{n-1}{N}, \frac{n}{N}\right]$. They are related to the corresponding Gaussian nodes $\tau_m, m = 0, 1, \ldots, M-1$ of the interval $[-1, 1]$ by the transformation

$$r_{nm} = \frac{1}{2N}(\tau_m + 2n - 1) \tag{2.7}$$

It can be shown that

$$s_{nm}\left(r_{ni}\right) = \delta_{mi} \tag{2.8}$$

and hence

$$c_{nm} = f\left(r_{nm}\right) \tag{2.9}$$

2.4. Numerical evaluation of single definite integral using Hybrid function

Consider the definite integral

$$\int_0^1 f(t)dt \tag{2.10}$$

Using Eq. (2.6) and Eq. (2.9), we have

$$\int_0^1 f(t)dt = \sum_{n=1}^{N}\sum_{m=0}^{M-1} f(r_{nm})w_{nm} \tag{2.11}$$

where $w_{nm} = \int_0^1 s_{nm}(t)dt$ are the weights which can be easily evaluated. It can be verified that

$$\sum_{n=1}^{N}\sum_{m=0}^{M-1} w_{nm} = 1 \tag{2.12}$$

Letting $t = a + (b-a)\,s$ in Eq. (2.10) leads to

$$\int_a^b f\left(t\right)dt = (b-a)\int_0^1 f\left(a + (b-a)\,s\right)ds \tag{2.13}$$

Using Eq. (2.11),

$$\int_a^b f\left(t\right)dt \approx (b-a)\sum_{n=1}^{N}\sum_{m=0}^{M-1} f\left(a + (b-a)\,r_{nm}\right)w_{nm} \tag{2.14}$$

2.5. Numerical evaluation of double definite integral using Hybrid function

Consider the double integral with variable limits of the type

$$\int_a^b \int_{c(s)}^{d(s)} f\left(t, s\right)dt\,ds \tag{2.15}$$

Applying Eq. (2.14) to the inner integral by treating the outer integration variable s as constant, the above equation can be written as,

$$\int_a^b \int_{c(s)}^{d(s)} f\left(t, s\right)dtds \approx \int_a^b (d(s)-c(s))\sum_{n=1}^{N}\sum_{m=0}^{M-1} f(c(s) + (d(s)-c(s))r_{nm}, s)w_{nm}ds \tag{2.16}$$

Letting

$$g(s) = (d(s) - c(s)) \sum_{n=1}^{N} \sum_{m=0}^{M-1} f(c(s) + (d(s) - c(s))r_{nm}, s)w_{nm} \tag{2.17}$$

and again applying Eq. (2.14) to the outer integral leads to

$$\int_a^b \int_{c(s)}^{d(s)} f(t,s)dtds \approx \int_a^b g(s)ds \approx (b-a) \sum_{p=1}^{N'} \sum_{q=0}^{M'-1} g(a+(b-a)r_{pq})w_{pq} \tag{2.18}$$

In the above equation, N' represents the number of partitions of the outer interval and M' denotes the order of Legendre polynomial in each partition. The total number of nodes considered in the t and s directions are NM and $N'M'$ respectively.

2.6. Numerical evaluation of definite triple integral using Hybrid function

The procedure considered in the above double integral can be extended to obtain the following result for the triple integral with variable limits.

$$\int_a^b \int_{c(s)}^{d(s)} \int_{k(s,t)}^{l(s,t)} f(u,t,s)dudtds \approx (b-a) \sum_{v=1}^{N''} \sum_{j=0}^{M''-1} h(a+(b-a)r_{vj})w_{vj} \tag{2.19}$$

where

$$h(s) = (d(s) - c(s)) \sum_{p=1}^{N'} \sum_{q=0}^{M'-1} g(c(s) + (d(s) - c(s))r_{pq}, s)w_{pq} \tag{2.20}$$

and

$$g(s,t) = (k(s,t) - l(s,t)) \sum_{n=1}^{N} \sum_{m=0}^{M-1} f(k(s,t) + (l(s,t) - k(s,t))r_{nm}, s, t)w_{nm} \tag{2.21}$$

Here, the total number of nodes considered in the u, t and s directions are NM, $N'M'$ and $N''M''$ respectively.

3. Results and Discussions

A few examples of the finite element results on the heat transfer from Reddy [7, 8] are considered for a comparison study. While quadrature methods are used in obtaining finite element solutions, we considered finite element results using the present hybrid of block-pulse function and Lagrange polynomial.

3.1. 1D Linear Transient Problem

A fin of unit length is initially kept at 1^0C. The left end of the fin is maintained at 0^0C while the right end is insulated with unit thermal energy stored in the area of the fin. Assuming the thermal conductivity over the area to be unity, the governing differential equation for the temperature distribution $u(x,t)$ can be written as

$$\frac{\partial u}{\partial t} - \frac{\partial^2 u}{\partial x^2} = 0 \tag{3.1}$$

defined in the domain, $0 < x < 1$. The boundary conditions are given by $u(0,t) = 0$, $\frac{\partial u}{\partial x}(1,t) = 0$ with the initial condition $u(x,0) = 1$. The decoupled formulation of the Finite Element Model is considered wherein the shape function is a function of spatial co-ordinates and the nodal variable is the function of time. In the decoupled formulation over a typical element e, the solution variable u^e in the weak formulation of the differential equation is approximated by

$$u^e = \sum_{i=1}^{n} N_i^e(x) u_i^e(t) \tag{3.2}$$

where N_i^e is the shape function at the i^{th} node of an element e with n nodes. Keeping the time variable t constant, the finite element model is derived the same as in the steady state problems known as semi-discretized finite element method.

The semi-discretized finite element equations of a typical element e can be obtained in the form

$$[M^e]\{\dot{u}\} + [K^e]\{u\} = 0 \tag{3.3}$$

where

$$K_{ij}^e = \int_{x_a}^{x_b} \frac{\partial N_i^e}{\partial x} \frac{\partial N_j^e}{\partial x} dx \tag{3.4}$$

$$M_{ij}^e = \int_{x_a}^{x_b} N_i^e N_j^e dx \tag{3.5}$$

are the elements of the matrices $[K^e]$ and $[M^e]$ respectively.

Here, $[K^e]$ and $[M^e]$ are referred as conduction matrix and mass matrix respectively and both the matrices are independent of time. x_a and x_b are the left and right node of the element e. Using the α - family of approximation for time, the fully discretized finite element equation can be obtained as

$$\left\{\alpha \Delta t[K^e] + [M^e]\right\}\left\{u^e\right\}_{s+1} = \left\{[M^e] - \Delta t(1-\alpha)[K^e]\right\}\left\{u^e\right\}_s \tag{3.6}$$

$\left\{u^e\right\}_s$ and $\left\{u^e\right\}_{s+1}$ represents the elemental nodal values at time s and s+1 respectively. The elements Eq. (3.4) and Eq. (3.5) of the elemental matrices $[K^e]$ and $[M^e]$ are obtained using the Hybrid functions.

Table 1: The values of N and M taken for different types of elements.

	$[K^e]$	$[M^e]$
Linear	$N = 1; M = 1$	$N = 1; M = 2$
Quadratic	$N = 1; M = 2$	$N = 1; M = 3$
Cubic	$N = 1; M = 3$	$N = 1; M = 4$

Table 2: A comparison of the finite element solutions for different meshes at x=1 obtained using the present hybrid functions with exact solution for $\Delta t = 0.05$ and $\alpha = 0.5$.

Time	2L	4L	2Q	4Q	1C	2C	4C	Exact
0	1	1	1	1	1	1	1	1
0.05	1.0359	0.9951	0.9942	0.9928	0.9178	0.9905	0.9925	0.9969
0.1	0.9279	0.9588	0.9551	0.9549	0.9663	0.947	0.9533	0.9493
0.15	0.8169	0.8639	0.8831	0.8725	0.8269	0.8646	0.87	0.8642
0.2	0.7176	0.7557	0.7633	0.7731	0.7551	0.765	0.7713	0.7723
0.25	0.6301	0.6759	0.6933	0.6855	0.6592	0.6801	0.6839	0.6854
0.3	0.5533	0.5906	0.6006	0.607	0.5872	0.5991	0.6054	0.6068
0.35	0.4858	0.5251	0.5394	0.5358	0.517	0.5331	0.5346	0.5367
0.4	0.4266	0.4608	0.471	0.4741	0.4579	0.4664	0.4729	0.4745
0.45	0.3746	0.4083	0.4201	0.4188	0.4042	0.4182	0.4178	0.4194
0.5	0.3289	0.3592	0.3687	0.3701	0.3574	0.3628	0.3693	0.3708
0.55	0.2888	0.3176	0.3275	0.3273	0.3158	0.3279	0.3264	0.3277
0.6	0.2536	0.2798	0.2883	0.289	0.2792	0.2824	0.2884	0.2897
0.65	0.2227	0.2472	0.2555	0.2556	0.2467	0.2569	0.2549	0.2561
0.7	0.1955	0.218	0.2253	0.2258	0.218	0.22	0.2253	0.2264
0.75	0.1717	0.1924	0.1995	0.1996	0.1927	0.2011	0.1991	0.2001
0.8	0.1508	0.1697	0.1761	0.1764	0.1703	0.1715	0.176	0.1769
0.85	0.1324	0.1498	0.1557	0.1559	0.1505	0.1574	0.1555	0.1563
0.9	0.1162	0.1322	0.1375	0.1378	0.133	0.1337	0.1375	0.1382
0.95	0.1021	0.1166	0.1216	0.1218	0.1176	0.123	0.1215	0.1222
1	0.0896	0.1029	0.1074	0.1076	0.1039	0.1044	0.1074	0.1080

Table 1 shows the values of M and N chosen for calculating the elements of $[K^e]$ and $[M^e]$, although the values of N and M may be chosen independently of each other.

The Finite Element Solutions at $x = 1$ for linear (L), quadratic (Q) and cubic (C) elements were obtained using Hybrid functions and compared with the exact solution $(Table\ 2)$. When α is taken as 0.5 and Δt as 0.05, the solutions are comparable up to two decimal places. Tables 3, 4 and 5 represents the finite element solutions for the temperature distribution of 12 linear elements, 6 quadratic elements and 4 cubic elements over the rectangular domain with spacings $\Delta x = 1/12$ and $\Delta t = 0.05$ for the $\alpha = 0.5$.

Fig. 1 (a) presents the comparison between forward scheme ($\alpha = 0$), backward scheme ($\alpha = 1$) and Crank-Nicolson scheme ($\alpha = 0.5$) for 2 linear and 1 quadratic finite elements. The exact solution is also presented in the same graph. We can infer that better approximation is obtained by Crank-Nicolson scheme than that of forward and backward scheme. The convergence of the finite element solution with increasing number of elements is obvious.

Fig. 1 (b) provides a comparison of the temperature distribution over the spatial

variable x at t=1 obtained from the data of Tables 3- 5. It is clear that slight discrepancies may exist as the order of element is increased for fixed spatial nodes.

Table 3: The finite element solutions for the temperature distribution of 12 linear elements with $\Delta t = 0.05$ and $\alpha = 0.5$.

Time/x	0	0.0833	0.1667	0.25	0.3333	0.4167	0.5	0.5833	0.6667	0.75	0.8333	0.9167	1
0	0	1	1	1	1	1	1	1	1	1	1	1	1
0.05	0	-0.2302	0.2783	0.5766	0.7516	0.8542	0.9144	0.9496	0.9702	0.982	0.9887	0.992	0.993
0.1	0	0.4472	0.2813	0.3469	0.4808	0.6153	0.7267	0.8109	0.8707	0.9111	0.9366	0.9506	0.955
0.15	0	-0.119	0.2699	0.4014	0.4738	0.5436	0.6178	0.6902	0.7541	0.8054	0.8422	0.8642	0.8715
0.2	0	0.2935	0.1499	0.2538	0.3795	0.4805	0.5584	0.621	0.6726	0.7145	0.7456	0.765	0.7715
0.25	0	-0.0685	0.237	0.2965	0.3445	0.4093	0.4788	0.5419	0.5939	0.6338	0.6619	0.6786	0.6841
0.3	0	0.2121	0.0957	0.2079	0.307	0.3767	0.4318	0.4802	0.5228	0.5581	0.5842	0.6002	0.6055
0.35	0	-0.0435	0.199	0.2206	0.2604	0.3188	0.3765	0.4253	0.4645	0.4948	0.5166	0.5299	0.5344
0.4	0	0.1593	0.0639	0.1714	0.2447	0.293	0.3346	0.3737	0.4083	0.4363	0.4566	0.4688	0.4728
0.45	0	-0.0302	0.1638	0.1642	0.2001	0.2505	0.2958	0.3326	0.3623	0.3859	0.4032	0.4139	0.4175
0.5	0	0.1223	0.043	0.1408	0.1929	0.227	0.2599	0.2916	0.3193	0.3411	0.3566	0.3659	0.369
0.55	0	-0.0226	0.1337	0.1221	0.1553	0.1972	0.2319	0.2596	0.2825	0.3011	0.3148	0.3233	0.3261
0.6	0	0.0952	0.0285	0.1153	0.151	0.1758	0.2024	0.228	0.2496	0.2664	0.2784	0.2857	0.2881
0.65	0	-0.0179	0.1089	0.0907	0.1213	0.1553	0.1814	0.2024	0.2203	0.235	0.2459	0.2525	0.2547
0.7	0	0.075	0.0182	0.0942	0.1175	0.1362	0.1579	0.1783	0.1951	0.208	0.2173	0.223	0.2249
0.75	0	-0.0149	0.0886	0.0671	0.0953	0.1222	0.1416	0.1578	0.1719	0.1836	0.192	0.1971	0.1988
0.8	0	0.0596	0.0109	0.0769	0.0911	0.1056	0.1234	0.1394	0.1524	0.1624	0.1697	0.1741	0.1756
0.85	0	-0.0127	0.0722	0.0493	0.0751	0.096	0.1104	0.123	0.1342	0.1434	0.15	0.1539	0.1552
0.9	0	0.0476	0.0057	0.0628	0.0704	0.0819	0.0965	0.109	0.119	0.1267	0.1325	0.136	0.1372
0.95	0	-0.0111	0.059	0.036	0.0594	0.0754	0.0861	0.0959	0.1048	0.112	0.1171	0.1202	0.1212
1	0	0.0384	0.0021	0.0514	0.0542	0.0637	0.0755	0.0852	0.0929	0.0989	0.1034	0.1062	0.1071

Table 4: The finite element solutions for the temperature distribution of 6 quadratic elements with $\Delta t = 0.05$ and $\alpha = 0.5$.

Time/x	0	0.0833	0.1667	0.25	0.3333	0.4167	0.5	0.5833	0.6667	0.75	0.8333	0.9167	1
0	1	1	1	1	1	1	1	1	1	1	1	1	1
0.05	0	-0.2036	0.3062	0.5905	0.7579	0.8571	0.9154	0.9499	0.9701	0.9819	0.9885	0.9918	0.9928
0.1	0	0.4164	0.2559	0.3443	0.486	0.6206	0.7309	0.8134	0.872	0.9116	0.9367	0.9504	0.9547
0.15	0	-0.0848	0.297	0.4039	0.4715	0.5435	0.6194	0.6925	0.7563	0.8071	0.8434	0.8651	0.8722
0.2	0	0.2604	0.1261	0.2555	0.3842	0.4824	0.5591	0.6215	0.6736	0.7158	0.7472	0.7666	0.7732
0.25	0	-0.0362	0.2601	0.2952	0.3425	0.4106	0.481	0.5438	0.5954	0.6351	0.6632	0.68	0.6855
0.3	0	0.1822	0.0753	0.2109	0.3096	0.3767	0.4319	0.4811	0.5242	0.5596	0.5857	0.6016	0.607
0.35	0	-0.0154	0.2183	0.2187	0.2604	0.321	0.3783	0.4265	0.4655	0.4959	0.5179	0.5313	0.5359
0.4	0	0.1338	0.0468	0.1742	0.2452	0.2924	0.3349	0.3749	0.4097	0.4377	0.4579	0.4701	0.4741
0.45	0	-0.0066	0.1801	0.1628	0.2018	0.2526	0.2971	0.3334	0.3632	0.3869	0.4044	0.4152	0.4188
0.5	0	0.101	0.0285	0.1428	0.1917	0.2265	0.2606	0.2929	0.3204	0.3422	0.3577	0.3671	0.3702
0.55	0	-0.0031	0.1476	0.1215	0.1582	0.199	0.2326	0.2602	0.2833	0.3021	0.3159	0.3244	0.3272
0.6	0	0.0778	0.0161	0.1164	0.1487	0.1756	0.2033	0.229	0.2505	0.2673	0.2794	0.2867	0.2891
0.65	0	-0.0019	0.1208	0.0907	0.125	0.1565	0.1817	0.2029	0.2211	0.236	0.2468	0.2534	0.2556
0.7	0	0.0607	0.0076	0.0946	0.1145	0.1362	0.1589	0.1792	0.1958	0.2088	0.2182	0.2239	0.2258
0.75	0	-0.0018	0.099	0.0676	0.0994	0.123	0.1418	0.1583	0.1727	0.1844	0.1928	0.1979	0.1996
0.8	0	0.0479	0.0016	0.0767	0.0876	0.1059	0.1243	0.1401	0.1529	0.163	0.1704	0.1749	0.1764
0.85	0	-0.002	0.0813	0.0502	0.0794	0.0964	0.1105	0.1235	0.1349	0.144	0.1506	0.1546	0.1559
0.9	0	0.0381	-0.0024	0.0623	0.0666	0.0825	0.0973	0.1095	0.1194	0.1273	0.1331	0.1366	0.1378
0.95	0	-0.0023	0.067	0.0371	0.0638	0.0755	0.0861	0.0964	0.1054	0.1125	0.1177	0.1207	0.1218
1	0	0.0306	-0.0051	0.0506	0.0503	0.0643	0.0762	0.0856	0.0932	0.0994	0.104	0.1067	0.1076

3.2. 2D Linear Transient Problem

An isotropic unit square slab is subjected to heat conduction with internal heat energy generation of $1W/m^3$. The left and the bottom of the slab are insulated while the top and right side of the slab are maintained at 0^0C. Initially, the slab is kept at 0^0C. Taking the conductivity of the medium to be unity, the governing differential equation for the temperature distribution $T(x, y, t)$ is

$$\frac{\partial T}{\partial t} - \left(\frac{\partial^2 T}{\partial x^2} + \frac{\partial^2 T}{\partial y^2} \right) = 1 \tag{3.7}$$

Table 5: The finite element solutions for the temperature distribution of 4 cubic elements with $\Delta t = 0.05$ and $\alpha = 0.5$.

Time/x	0	0.0833	0.1667	0.25	0.3333	0.4167	0.5	0.5833	0.6667	0.75	0.8333	0.9167	1
0	1	1	1	1	1	1	1	1	1	1	1	1	1
0.05	0	-0.2169	0.2808	0.5678	0.7451	0.8495	0.9109	0.9473	0.9686	0.9809	0.9879	0.9914	0.9925
0.1	0	0.4295	0.2834	0.3656	0.4902	0.6191	0.7274	0.8099	0.8691	0.9093	0.9348	0.9488	0.9533
0.15	0	-0.0982	0.2655	0.3786	0.4664	0.5427	0.6191	0.6914	0.7546	0.805	0.8412	0.8628	0.87
0.2	0	0.2715	0.1569	0.2796	0.3853	0.4799	0.5564	0.6196	0.672	0.7142	0.7454	0.7647	0.7713
0.25	0	-0.0461	0.2285	0.2693	0.3407	0.4109	0.4806	0.5424	0.5937	0.6334	0.6615	0.6783	0.6839
0.3	0	0.1899	0.1054	0.2356	0.309	0.3745	0.4303	0.48	0.5231	0.5583	0.5842	0.6	0.6054
0.35	0	-0.0218	0.1885	0.193	0.26	0.3212	0.3776	0.4252	0.4641	0.4946	0.5166	0.53	0.5346
0.4	0	0.1384	0.0748	0.1986	0.244	0.2908	0.334	0.3741	0.4088	0.4366	0.4567	0.4688	0.4729
0.45	0	-0.0101	0.1527	0.1378	0.202	0.2527	0.2963	0.3323	0.3622	0.386	0.4035	0.4141	0.4178
0.5	0	0.1032	0.0541	0.1666	0.1904	0.2254	0.26	0.2923	0.3196	0.3413	0.3568	0.3661	0.3693
0.55	0	-0.0045	0.1229	0.0974	0.1586	0.1988	0.232	0.2594	0.2826	0.3014	0.3152	0.3236	0.3264
0.6	0	0.0782	0.0392	0.1392	0.1475	0.1749	0.2028	0.2285	0.2499	0.2666	0.2787	0.2859	0.2884
0.65	0	-0.0019	0.0987	0.0679	0.1253	0.1562	0.1813	0.2024	0.2206	0.2354	0.2462	0.2528	0.2549
0.7	0	0.06	0.0282	0.1163	0.1136	0.1359	0.1584	0.1787	0.1952	0.2082	0.2176	0.2233	0.2253
0.75	0	-0.0007	0.0793	0.0461	0.0996	0.1226	0.1416	0.1579	0.1723	0.1839	0.1923	0.1974	0.1991
0.8	0	0.0464	0.0199	0.0972	0.0871	0.1058	0.1237	0.1397	0.1525	0.1626	0.17	0.1745	0.176
0.85	0	-0.0004	0.0639	0.0301	0.0794	0.0959	0.1107	0.1233	0.1346	0.1437	0.1502	0.1542	0.1555
0.9	0	0.0362	0.0137	0.0814	0.0664	0.0825	0.0965	0.1091	0.1191	0.127	0.1328	0.1363	0.1375
0.95	0	-0.0004	0.0516	0.0184	0.0636	0.075	0.0865	0.0963	0.1052	0.1122	0.1174	0.1204	0.1215
1	0	0.0285	0.0091	0.0684	0.0504	0.0645	0.0753	0.0853	0.093	0.0992	0.1037	0.1064	0.1074

defined in the domain $0 \leq x \leq 1,\ 0 \leq y \leq 1$. The boundary conditions are given as $\frac{\partial T}{\partial x}(0, y, t) = 0,\ \frac{\partial T}{\partial y}(x, 0, t) = 0,\ T(1, y, t) = 0$ and $T(x, 1, t) = 0$ with the initial condition $T(x, y, 0) = 0 \quad \forall (x, y)$ defined in the domain.

The decoupled formulation of the Finite Element Model is considered over a typical element e, in which, the solution variable T^e in the weak formulation of the differential equation Eq. (3.7) is approximated by

$$T^e = \sum_{i=1}^{n} \psi_i^e(x, y) T_i^e(t) \tag{3.8}$$

where $\psi_i^e(x, y)$ is the shape function at the i^{th} node of an element e with n nodes. Keeping the time variable t constant, the semi-discretized finite element equation is given by

$$[M^e]\left\{\dot{T}\right\} + [K^e]\{T\} = \left\{f^e\right\} + \left\{Q^e\right\} \tag{3.9}$$

where

$$M_{ij}^e = \int_{y_a}^{y_b}\int_{x_a}^{x_b} \psi_i^e \psi_j^e dxdy = \int_0^1 \int_0^{1-L_2} L_i^e L_j^e |J| dL_1 dL_2 \tag{3.10}$$

$$\begin{aligned} K_{ij}^e &= \int_{y_a}^{y_b}\int_{x_a}^{x_b} \left(\frac{\partial \psi_i^e}{\partial x}\frac{\partial \psi_j^e}{\partial x} + \frac{\partial \psi_i^e}{\partial y}\frac{\partial \psi_j^e}{\partial y}\right) dxdy \\ &= \int_0^1 \int_0^{1-L_2} \left[\left(J_{11}^* \frac{\partial L_i^e}{\partial \xi} + J_{12}^* \frac{\partial L_i^e}{\partial \eta}\right)\left(J_{11}^* \frac{\partial L_j^e}{\partial \xi} + J_{12}^* \frac{\partial L_j^e}{\partial \eta}\right)\right. \\ &\quad \left. + \left(J_{21}^* \frac{\partial L_i^e}{\partial \xi} + J_{22}^* \frac{\partial L_i^e}{\partial \eta}\right)\left(J_{21}^* \frac{\partial L_j^e}{\partial \xi} + J_{22}^* \frac{\partial L_j^e}{\partial \eta}\right)\right] |J| dL_1 dL_2 \end{aligned} \tag{3.11}$$

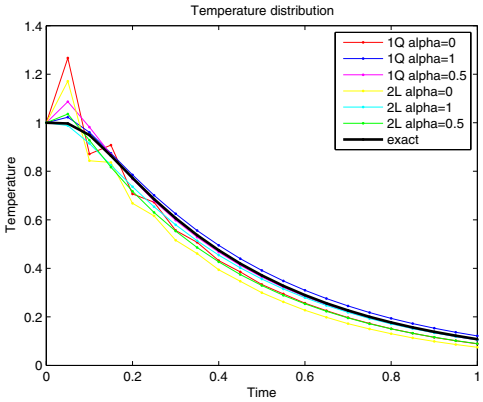

(a) Comparison between different schemes according to linear and quadratic elements

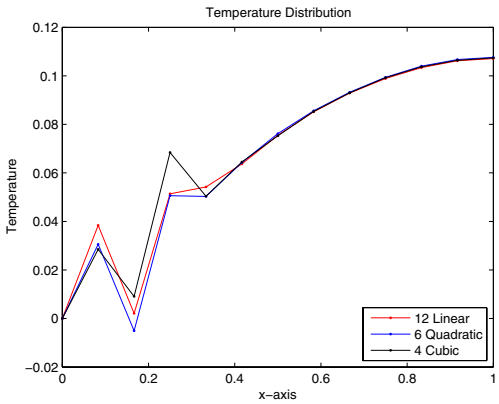

(b) Temperature Distribution at one minute

Figure 1: 1D Linear Transient.

$$
\begin{aligned}
f_i^e &= \int_{y_a}^{y_b} \int_{x_a}^{x_b} \psi_i^e dxdy + \oint_{\Gamma^e} q_n \psi_i^e d\Gamma \\
&= \int_0^1 \int_0^{1-L_2} L_i^e |J| dL_1 dL_2 + \oint_{\Gamma^e} q_n L_i^e |J| d\Gamma
\end{aligned} \tag{3.12}
$$

In which, q_n is the secondary boundary condition over the boundary Γ^e of the element e. And, x_a and x_b are the left and right end on the x-axis of the element; y_a and y_b are the top and bottom on the y-axis of the element. L_i^e ,$i = 1, 2, 3$ are the interpolation

functions in area co-ordinates. Here, $L_3^e = 1 - L_1^e - L_2^e$ and the Jacobian matrix,

$$[J] = \begin{bmatrix} \dfrac{\partial x}{\partial L_1^e} & \dfrac{\partial y}{\partial L_1^e} \\ \dfrac{\partial x}{\partial L_2^e} & \dfrac{\partial y}{\partial L_2^e} \end{bmatrix} \tag{3.13}$$

$$[J]^{-1} \equiv [J^*] = \begin{bmatrix} J_{11}^* & J_{12}^* \\ J_{21}^* & J_{22}^* \end{bmatrix} \tag{3.14}$$

The variable limits in the integrals are evaluated using Hybrid function. The α - family of time approximation is considered and the fully discretized Finite Element Equations for the problem is presented as,

$$\begin{aligned} \left\{\alpha \Delta t[K^e] + [M^e]\right\} \left\{u^e\right\}_{s+1} = \left\{[M^e] - \Delta t(1-\alpha)[K^e]\right\} \left\{u^e\right\}_s \\ + \Delta t \left[(1-\alpha) \left\{F^e\right\}_s + \alpha \left\{F^e\right\}_{s+1}\right] \end{aligned} \tag{3.15}$$

Fig. 2 shows the domain as a 2-D mesh divided into 32 linear triangular elements. The matrices for each element are evaluated using Hybrid functions by taking $N = 1, M = 1; N^{'} = 1, M^{'} = 1$ for $[K^e]$; $N = 1, M = 2; N^{'} = 1, M^{'} = 2$ for $[M^e]$; $N = 1, M = 2; N^{'} = 1, M^{'} = 2$ for $\left\{F^e\right\}$. Table 6 presents a numerical comparison of the finite element results between the forward scheme ($\alpha = 0$) and the Crank-Nicolson scheme ($\alpha = 0.5$) at each mesh point with the time step $\Delta t = 0.05$, at a given time t=1.

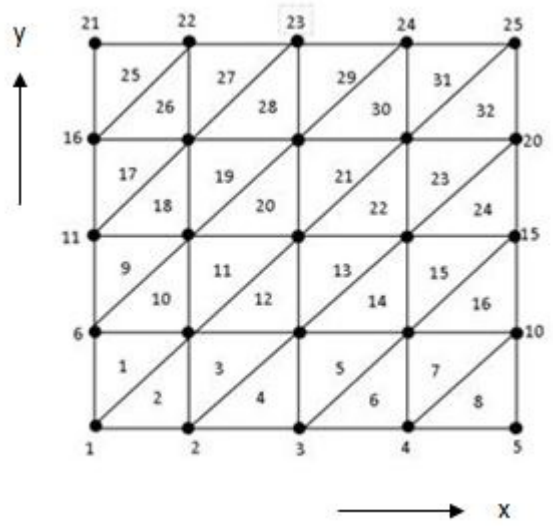

Figure 2: Finite Element 2-D Mesh

The solutions are comparable with that of the classical quadrature method up to 4 decimal places. Fig. 3 shows a comparison of the finite element solutions of the temporal

Table 6: Comparison of the finite element results between the schemes of a 2-D mesh at time $t = 1$.

Nodes	**1**	**2**	**3**	**4**	**5**	**6**	**7**	**8**	**9**	**10**
$\alpha = 0.5$	0.2992	0.2786	0.2277	0.1385	0	0.2786	0.2627	0.2159	0.1319	0
$\alpha = 0$	0.2993	0.2787	0.2278	0.1385	0	0.2787	0.2628	0.216	0.132	0
Nodes	**11**	**12**	**13**	**14**	**15**	**16**	**17**	**8**	**19**	**20**
$\alpha = 0.5$	0.2277	0.2159	0.179	0.1111	0	0.1385	0.1319	0.1111	0.0712	0
$\alpha = 0$	0.2278	0.216	0.1791	0.1111	0	0.1385	0.132	0.1111	0.0712	0
Nodes	**21**	**22**	**23**	**24**	**25**					
$\alpha = 0.5$	0	0	0	0	0					
$\alpha = 0$	0	0	0	0	0					

temperature distribution at the mesh points (0.25, 0.25) , (0, 0.5) and (0.5, 0.5) obtained using the present hybrid function(denoted by $*$) and quadrature method (denoted by o) by taking $\alpha = 0.5$ and $\Delta t = 0.05$. It is clear that the finite elements are in good agreement with the corresponding results obtained using quadrature method.

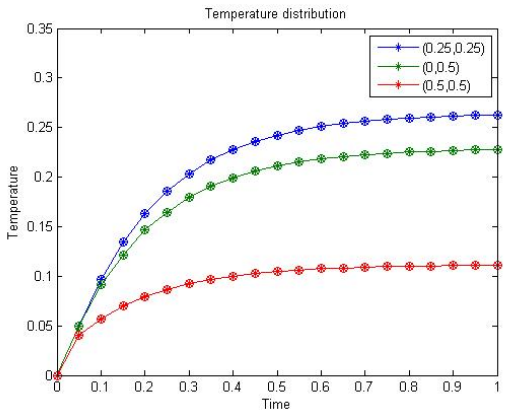

Figure 3: Temperature Distribution at certain points

3.3. 2D Nonlinear Steady State Problem

An isotropic rectangular slab of dimension 0.18 x $0.1m$ is subjected to heat conduction. The thermal conductivity of the slab material is taken to be a linear function of temperature, i.e. $k = k_0(1 + \beta T)$; where k_0 is the constant thermal conductivity, β the temperature of thermal conductivity, and T is the temperature. The left side of the slab is maintained at 500 K and the right side at 300K. There is no internal heat generation in the slab. The governing differential equation for the temperature distribution $T(x, y)$ is,

$$-\frac{\partial}{\partial x}\left[k_0(1+\beta T)\frac{\partial T}{\partial x}\right] - \frac{\partial}{\partial y}\left[k_0(1+\beta T)\frac{\partial T}{\partial y}\right] = 0 \tag{3.16}$$

Defined in the domain, $0 < x < 0.18, 0 < y < 0.1$ for the boundary conditions $T(0, y) = 500K$, $T(0.18, y) = 300K$, and $\dfrac{\partial T}{\partial y} = 0$ at $y = 0, b$ for any x.

The solution variable,

$$T^e = \sum \psi_i^e(x, y) T_i^e \tag{3.17}$$

is applied to the weak form of the differential equation Eq. (3.16) to obtain the finite element equation, which is given by,

$$[K^e(T)]\{T\} = \left\{Q^e\right\} \tag{3.18}$$

where

$$\begin{aligned} K_{ij}^e &= \int\int_{\Omega_e} \left\{ k_0 \left[1 + \beta \left(\sum \psi_j^e T_j^e \right) \right] \left[\frac{\partial \psi_i^e}{\partial x} \frac{\partial \psi_j^e}{\partial x} + \frac{\partial \psi_i^e}{\partial y} \frac{\partial \psi_j^e}{\partial y} \right] \right\} dxdy \\ &= \int_{-1}^{1}\int_{-1}^{1} \left\{ k_0 \left[1 + \beta \left(\sum \psi_j^e T_j^e \right) \right] \left[\left(J_{11}^* \frac{\partial \psi_i^e}{\partial \xi} + J_{12}^* \frac{\partial \psi_i^e}{\partial \eta} \right) \left(J_{11}^* \frac{\partial \psi_j^e}{\partial \xi} \right. \right. \right. \\ &\left. \left. \left. + J_{12}^* \frac{\partial \psi_j^e}{\partial \eta} \right) + \left(J_{21}^* \frac{\partial \psi_i^e}{\partial \xi} + J_{22}^* \frac{\partial \psi_i^e}{\partial \eta} \right) \left(J_{21}^* \frac{\partial \psi_j^e}{\partial \xi} + J_{22}^* \frac{\partial \psi_j^e}{\partial \eta} \right) \right] \right\} |J| d\xi d\eta \end{aligned}$$

$$Q_i^e = \oint_{\Gamma^e} \psi_i^e v d\Gamma \tag{3.19}$$

Ω_e and Γ^e are the domain and boundary of an element e and q_n is the secondary boundary condition. ψ_i^e represents the shape function at the i^{th} node of an element e with n nodes. $|J|$ denotes the determinant of the Jacobian, and the Jacobian matrix is given by

$$[J] = \begin{bmatrix} \dfrac{\partial x}{\partial \xi} & \dfrac{\partial y}{\partial \xi} \\ \dfrac{\partial x}{\partial \eta} & \dfrac{\partial y}{\partial \eta} \end{bmatrix} \tag{3.20}$$

and

$$[J]^{-1} \equiv [J^*] = \begin{bmatrix} J_{11}^* & J_{12}^* \\ J_{21}^* & J_{22}^* \end{bmatrix} \tag{3.21}$$

$$dA \equiv dx\, dy = |J|\, d\xi\, d\eta \tag{3.22}$$

For the finite element analysis of the temperature distribution, 4 x 4 meshes of four-node linear rectangular elements were considered (shown in Fig. 4).

The element conductivity matrix, K_{ij}^e is numerically evaluated by hybrid function with $N = 1, M = 1; N^{'} = 1, M^{'} = 1$. The finite element solution thus obtained are presented in Table 7 which are the same as those obtained by quadrature method. The solution converged with less number of iterations when compared with the quadrature method.

From Table 7 we can infer that the temperature for any y when $x = 0$ (the left side of the slab) is 500 K and the temperature when $x = 0.18$ for any y (the right side of the slab) is 300K. Inside the slab, the temperature varies steadily.

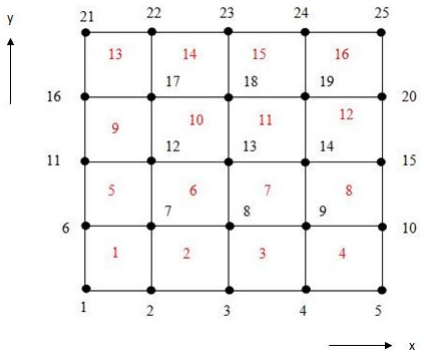

Figure 4: 2-D Mesh for the Nonlinear Problem

Table 7: Finite element solution obtained using the present hybrid method

Nodes	**1**	**2**	**3**	**4**	**5**	**6**	**7**	**8**	**9**	**10**
Temperatures	500	454	406	354	300	500	454	406	354	300
Nodes	**11**	**12**	**13**	**14**	**15**	**16**	**17**	**8**	**19**	**20**
Temperatures	500	454	406	354	300	500	454	406	354	300
Nodes	**21**	**22**	**23**	**24**	**25**					
Temperatures	500	454	406	354	300					

3.4. 3-D Linear Steady State Problem

An isotropic slab of dimensions 1 x 1 x 10m is considered for the analysis, in which the left face is maintained at a temperature of 100^0C while the bottom, top and right faces are maintained at 0^0C. The front and back faces are assumed to be insulated and there is no internal heat generation (Fig. 5).

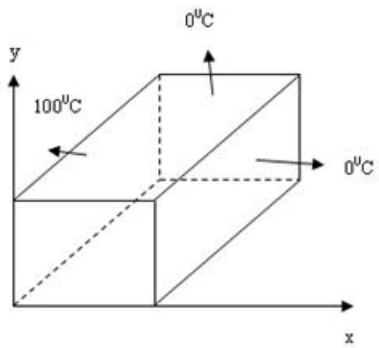

Figure 5: Geometry and boundary conditions

Since only temperature boundary conditions are involved, the solution will be independent of the conductivity of the medium. The governing differential equation of the

temperature $T(x, y, z)$ is given by

$$-\frac{\partial}{\partial x}\left(k_x \frac{\partial T}{\partial x}\right) - \frac{\partial}{\partial y}\left(k_y \frac{\partial T}{\partial y}\right) - \frac{\partial}{\partial z}\left(k_z \frac{\partial T}{\partial z}\right) = g \tag{3.23}$$

defined in the domain $0 < x < 1, 0 < y < 1, 0 < z < 10$; where g is the internal heat generation, which is equal to zero for this problem. Since isotropic material is considered, k_x, k_y, k_z are same and is unity. Due to symmetry, a quadrant of the domain (1 x 0.5 x 5 m) is modeled using a 4 x 2 x 2 mesh of eight-node brick elements (Fig. 6).

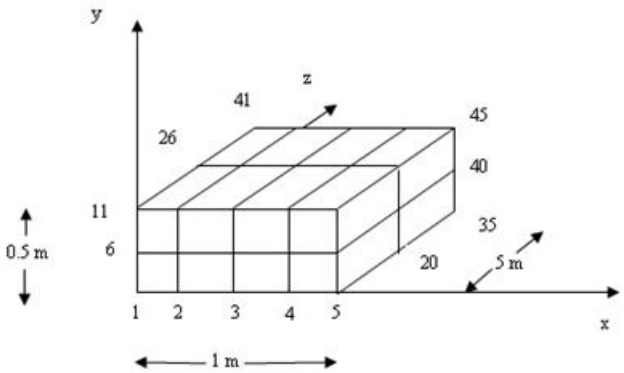

Figure 6: 3-D Computational domain

Using the approximate solution,

$$T^e = \sum \psi_i^e(x, y, z) T_i^e \tag{3.24}$$

for the weak formulation of the differential equation Eq. (3.23), the finite element equation is given as

$$[K^e]\{T\} = 0 \tag{3.25}$$

where

$$K_{ij}^e = \int_{\Omega^e} \left(\frac{\partial \psi_i^e}{\partial x}\frac{\partial \psi_j^e}{\partial x} + \frac{\partial \psi_i^e}{\partial y}\frac{\partial \psi_j^e}{\partial y} + \frac{\partial \psi_i^e}{\partial z}\frac{\partial \psi_j^e}{\partial z} \right) dV \tag{3.26}$$

In which, ψ_i^e are the shape functions at the i^{th} node of an element e with n nodes and

$$x = \sum_{i=1}^{3} x_i \psi_i^e(\xi, \eta, \zeta),\ y = \sum_{i=1}^{3} y_i \psi_i^e(\xi, \eta, \zeta),\ z = \sum_{i=1}^{3} z_i \psi_i^e(\xi, \eta, \zeta) \tag{3.27}$$

The transformation from Cartesian co-ordinates to Natural co-ordinates is carried out

using the relation,

$$\begin{Bmatrix} \frac{\partial \psi_i^e}{\partial x} \\ \frac{\partial \psi_i^e}{\partial y} \\ \frac{\partial \psi_i^e}{\partial z} \end{Bmatrix} = [J]^{-1} \begin{Bmatrix} \frac{\partial \psi_i^e}{\partial \xi} \\ \frac{\partial \psi_i^e}{\partial \eta} \\ \frac{\partial \psi_i^e}{\partial \zeta} \end{Bmatrix} \tag{3.28}$$

where the Jacobian matrix is given by,

$$[J] = \begin{bmatrix} \frac{\partial x}{\partial \xi} & \frac{\partial y}{\partial \xi} & \frac{\partial z}{\partial \xi} \\ \frac{\partial x}{\partial \eta} & \frac{\partial y}{\partial \eta} & \frac{\partial z}{\partial \eta} \\ \frac{\partial x}{\partial \zeta} & \frac{\partial y}{\partial \zeta} & \frac{\partial z}{\partial \zeta} \end{bmatrix} \tag{3.29}$$

The temperature field obtained using the present hybrid function method is depicted in Table 8. All the planes parallel to the plane $z = 0$ have the same temperature distribution, as the 3-D solution is same as the 2-D solution on assuming that the slab is infinitely long in the z-direction. The finite element solution obtained (Table 8) was same as that obtained using the Gauss quadrature method when we take $N = 3, M = 2; N^{'} = 3, M^{'} = 2; N^{''} = 3, M^{''} = 2$.

Table 8: Temperature field for the 3-D mesh

Nodes	**1**	**2**	**3**	**4**	**5**	**6**	**7**	**8**	**9**	**10**	**11**	**12**	**13**	**14**	**15**
Temperature	100	0	0	0	0	100	50.7	19.29	7.15	0	100	58.48	27.86	10.09	0
Nodes	**16**	**17**	**18**	**19**	**20**	**21**	**22**	**23**	**24**	**25**	**26**	**27**	**28**	**29**	**30**
Temperature	100	0	0	0	0	100	50.7	19.29	7.15	0	100	58.48	27.86	10.09	0
Nodes	**31**	**32**	**33**	**34**	**35**	**36**	**37**	**38**	**39**	**40**	**41**	**42**	**43**	**44**	**45**
Temperature	100	0	0	0	0	100	50.7	19.29	7.15	0	100	58.48	27.86	10.09	0

4. Conclusion

Finite element solutions can be obtained using the hybrid of Block-Pulse function and Lagrange polynomial. The procedure is illustrated by considering heat conduction problems of 1-D, 2-D and 3-D; linear and nonlinear; steady state and transient problems. The present method can be used to obtain accurate results as illustrated in the results presented. A comparison study with the corresponding finite element solutions obtained using the traditional Gauss quadrature method shows that the present method is comparable and in good agreement.

References

[1] Siraj-ul-Islam, Aziz, I., and Haq, F., 2010, "A comparative study of numerical integration based on haar wavelets and hybrid function," Computers and Mathematics with Applications, 59, pp. 2026–2036.

[2] Uma, G., Prabhakar, V., and Hariharan, S., 2014, "A quadrature rule for numerical integration using hybrid of block-pulse functions and lagrange polynomial," Proc. of National Conference on Pure and Applied Mathematics,(NCPAM '14), Chennai, India, pp. 142–146.

[3] Marzban, H.R., Tabrizidooz, H.R., and Razzaghi, M., 2008, "Hybrid function for non-linear initial value problems with applications to lane-emden type equations," Physics Letters A, 372, pp. 5883–5886.

[4] Marzban, H.R., Hoseini, S.M., and Razzaghi, M., 2009, "Solution of the volterra's population model via block-pulse functions and lagrange-interpolating polynomials," Mathematical Methods in the Applied Sciences, 32, pp. 127–134.

[5] Marzban, H.R., and Hoseini, S.M., 2012, "Solution of nonlinear volterra-fredholm integro-differential equations via hybrid of block-pulse functions and lagrange interpolating polynomials," Advances in Numerical Analysis, pp. 1-14.

[6] Marzban, H.R., Tabrizidooz, H.R., and Razzaghi, M., 2008, "Solution of variational problems via hybrid of block-pulse and lagrange interpolating," IET Control theory and Applications, 3, pp. 1363–1369.

[7] Reddy, J.N., 2005, An introduction to the Finite Element Method, McGraw Hill Education(India) Pvt. Ltd., India.

[8] Reddy, J.N., 2008, An introduction to Nonlinear Finite Element Analysis, Oxford University Press, India.